JOURNAL OF BACTERIOLOGY, Feb. 2000, p. 1035–1045 Vol. 182, No. 4
0021-9193/00/$04.00+0
Copyright © 2000, American Society for Microbiology. All Rights Reserved.

Insertional Inactivation of Genes Encoding Components of the Sodium-Type Flagellar Motor and Switch of *Vibrio parahaemolyticus*

BLAISE R. BOLES AND LINDA L. MCCARTER*

Department of Microbiology, University of Iowa, Iowa City, Iowa 52242

Received 18 August 1999/Accepted 24 November 1999

Vibrio parahaemolyticus **possesses two types of flagella, polar and lateral, powered by distinct energy sources, which are derived from the sodium and proton motive forces, respectively. Although proton-powered flagella in *Escherichia coli* and *Salmonella enterica* serovar Typhimurium have been extensively studied, the mechanism of torque generation is still not understood. Molecular knowledge of the structure of the sodium-driven motor is only now being developed. In this work, we identify the switch components, FliG, FliM, and FliN, of the sodium-type motor. This brings the total number of genes identified as pertinent to polar motor function to seven. Both FliM and FliN possess charged domains not found in proton-type homologs; however, they can interact with the proton-type motor of *E. coli* to a limited extent. Residues known to be critical for torque generation in the proton-type motor are conserved in the sodium-type motor, suggesting a common mechanism for energy transfer at the rotor-stator interface regardless of the driving force powering rotation. Mutants representing a complete panel of insertionally inactivated switch and motor genes were constructed. All of these mutants were defective in sodium-driven swimming motility. Alkaline phosphatase could be fused to the C termini of MotB and MotY without abolishing motility, whereas deletion of the unusual, highly charged C-terminal domain of FliM disrupted motor function. All of the mutants retained proton-driven, lateral motility over surfaces. Thus, although central chemotaxis genes are shared by the polar and lateral systems, genes encoding the switch components, as well as the motor genes, are distinct for each motility system.**

Vibrio parahaemolyticus is an organism with two distinct motility systems, adapted for life in different circumstances (42). The polar flagellar system (Fla) propels the bacterium in liquid environments (swimming motility), and the lateral flagellar (Laf) system moves the bacterium through viscous environments and over surfaces (swarming motility). The polar flagellar filament of the swimmer cell comprises multiple flagellin subunits and is sheathed by what appears, in the electron microscope, to be an extension of the cell outer membrane (41). This flagellum is produced constitutively, i.e., it is found on liquid- and surface-grown bacteria. In liquid medium, the rotating flagellum can propel the bacterium at speeds as fast as 60 μm per s (3). Although an effective propulsive organelle in dilute liquid environments, the polar flagellum of *V. parahaemolyticus* does not work well in viscous layers. Growth on surfaces or in viscous environments leads to induction of the alternate motility system and elaboration of numerous peritrichous flagella.

It is hypothesized that the polar flagellum serves not only as a propulsive organelle but also as a tactile sensor, informing the bacterium of contact with surfaces or viscous environments. Conditions that impede rotation of the polar flagellum lead to induction of the second motility system (38). Lateral flagella are produced solely under conditions that restrict the function of the polar flagellum. The lateral filaments are unsheathed and polymerized from a single flagellin subunit, which is distinct from the polar flagellins (44). Lateral flagella enable the bacterium to move over and colonize surfaces or viscous layers.

Energy to drive flagellar rotation is derived from the transmembrane electrochemical potential of specific ions (20, 28, 36). Rotation of the flagellum appears tightly coupled to the flow of ions through the motor (45). Two kinds of motors, which are dependent on different coupling ions, have been described: H^+- and Na^+-driven motors. In *V. parahaemolyticus*, the proton motive force powers the lateral flagella, whereas the sodium motive force drives polar flagellar rotation (3).

Proton-type motors of *Escherichia coli* and *Salmonella enterica* serovar Typhimurium have been extensively characterized (reviewed in references 5, 6, 13, and 32). The stator of this motor comprises two cytoplasmic membrane proteins, MotA and MotB (11, 54). Together, these proteins possess five transmembrane domains, which form a proton-conducting channel (7, 8, 51, 55, 66, 68). MotB contains a C-terminal domain that may fasten the MotA-MotB complex to peptidoglycan (10, 12). Multiple MotA-MotB torque-generating units surround the flagellar basal body (25). Torque is transmitted from the MotA-MotB stator to the rotor. Although the mechanism of torque generation is not understood, electrostatic interactions between specific, charged residues in MotA and FliG have been demonstrated (29, 30, 67). FliG is found at the base of the flagellar basal body in the switch complex with FliM and FliN (15, 46). This complex is essential for torque generation, flagellar assembly, and control of the direction of flagellar rotation (21, 53, 56, 57, 61, 64, 65).

The architecture of sodium-type motors of two marine *Vibrio* species, *V. parahaemolyticus* and *V. alginolyticus*, is currently being dissected. Four components of the stator have been described: MotX, MotY, MotA, and MotB. Transposon insertions in *motX* or *motY* of *V. parahaemolyticus* produce flagellated but nonmotile bacteria (39, 40). Other paralyzed mutants, which were generated by chemical mutagenesis, were isolated in *V. alginolyticus*. The lesions identified a new locus

* Corresponding author. Mailing address: Department of Microbiology, University of Iowa, Iowa City, IA 52242. Phone: (319) 335-9721. Fax: (319) 335-7679. E-mail: linda-mccarter@uiowa.edu.

containing two genes, designated *pomA* and *pomB* (2). For *V. parahaemolyticus*, a similar locus was discovered and designated *motAB* (GenBank accession no., AF069391) (22). The proteins derived from these two loci are greater than 96% identical. With respect to function and predicted protein topology, the *Vibrio* proteins resemble MotA and MotB of the proton-type motor, whereas MotX and MotY are unique to the sodium-type motor. The existence of mutants with alterations in *motA* or *motB* conferring resistance to sodium channel inhibitors that block motility provides strong evidence for roles for both of these proteins in Na^+ translocation (22, 26). MotY possesses a potentially extensive C-terminal peptidoglycan interaction domain (39). The function of MotX is a mystery. The switch components of the sodium-type motor, although presumed to exist, have not been identified until now.

Thus, the lateral and polar flagellar filaments are different, and the torque-generating units are distinct; however, a common chemotaxis system directs both forms of motility. Defects in chemotaxis genes affect both swimming and swarming motility (48). At times the bacterium elaborates both forms of flagella. Chemotaxis, specifically the modulation of direction of flagellar rotation, is effected through interaction of chemotaxis proteins with the switch complex. In *E. coli* and many other bacteria, phosphorylated CheY interacts with FliM (53, 60, 61, 62). What determines specificity with respect to assembly, function, and coordination of movement has not been determined, i.e., it is not known at what level divergence between the two motility systems occurs. This work describes the isolation and characterization of three newly identified polar flagellar switch genes, *fliG*, *fliM*, and *fliN*. Although mutations causing altered *V. parahaemolyticus* MotA or MotB function have been previously described (22), insertional inactivation of these genes had not been performed. Therefore, a complete panel of loss-of-function mutants, with insertions in each of the known switch and motor genes, was constructed to probe motor function and specificity of the gene products with respect to swimming and swarming motility.

MATERIALS AND METHODS

Bacterial strains and growth conditions. The strains and plasmids used in this work are described in Table 1. *Vibrio* strains were cultured at 30°C. All *V. parahaemolyticus* strains were derived from the wild-type strain BB22 (4). Strain LM1017 contains a mutation in the lateral flagellar hook gene and is unable to swarm (44). *E. coli* flagellar strains were derived from DFB9 and were provided by David Blair. HI broth contained 25 g of heart infusion broth (Difco) and 20 g of NaCl per liter. Solidified swarming medium was prepared by adding 15 g of Bacto agar (Difco) per liter to HI broth. Semisolid motility medium (M agar) contained 10 g of tryptone and 3.25 g of agar per liter; the medium also contained 20 g of NaCl/liter for *Vibrio* and 10 g of NaCl/liter for *E. coli*.

Mutant isolation. Isolation of mini-Mu mutant strain ML199, which is nonmotile and which produces no flagella, has been described previously (38). Specific mutations were created on plasmids in *E. coli* and then transferred to *V. parahaemolyticus* by allelic replacement. Plasmids were mutagenized with λTn*phoA* (35) or λTn*lacZ*/in (34). The precise point of insertion was defined by DNA sequencing. The procedures for conjugation and gene replacement in *V. parahaemolyticus* have been described elsewhere (52). General DNA manipulations were adapted from the methods of Sambrook et al. (47). All strain constructions were confirmed by Southern blot analysis of restricted chromosomal DNA. Chromosomal DNA was prepared according to the protocol of Woo et al. (63).

Retrieval of clones and plasmid construction. The *fliF* locus was identified by cloning a tetracycline-resistant transposon from the mini-Mu-induced Fla$^-$ mutant strain ML199 according to procedures described previously (52). The segment of chromosomal DNA contiguous with the transposon was sequenced and then used as a probe to retrieve cosmid pLM2047 from a *V. parahaemolyticus* library constructed using DNA prepared from strain BB22. Because cosmid pLM2047 contains more than 25 kb of *V. parahaemolyticus* DNA, the switch genes were subcloned for mutagenesis. For product identification and complementation, the switch genes were amplified by high-fidelity PCR (Boehringer Mannheim) and cloned into the isopropyl-β-D-thiogalactopyranoside (IPTG)-inducible expression vector pLM1877. Gentamicin-resistant plasmid pLM1877 is a broad-host-range, low-copy-number vector that was derived from vector pMMB66EH (17). PCR-generated clones were sequenced to verify fidelity.

***E. coli* minicell system.** Minicells were made from strain P678-54 as described by Engebrecht and Silverman (14). Plasmids were introduced by transformation. Minicells were prepared from 400 ml of an overnight culture grown in Luria broth with the appropriate antibiotic. The final pellet of purified minicells was suspended in 0.5 ml. Minicells (0.25 ml) were incubated for 20 min at 37°C, and then 20 μCi (1 Ci = 38.7 GBq) of [^{35}S]methionine with a specific activity of ~1,000 Ci/mmol (Amersham Life Sciences) was added. After continued incubation for 20 min, cells were pelleted and suspended in electrophoresis sample buffer. Details of Tris-glycine sodium dodecyl sulfate-polyacrylamide gel electrophoresis (SDS-PAGE) have been described previously (43). Fixed and stained gels were incubated with Amplify reagent (Amersham) before drying and autoradiography. The resolving gel was 10.5% acrylamide. Broad-range SDS-PAGE protein standards were purchased from Bio-Rad (Hercules, Calif.).

Immunoblot analysis. SDS-PAGE was conducted as described above. Resolving gels contained 12% acrylamide. Gels were transferred to a polyvinylidene difluoride membrane (Immobilon-P; Millipore Corp.) in transfer buffer containing 12.5 mM Tris base, 96 mM glycine, and 20% methanol for 90 min at 30 V. After being blocked in TBST buffer (10 mM Tris-Cl [pH 8], 0.15 M NaCl, 0.05% Tween 20) containing 5% nonfat dry milk, blots were incubated in TBST buffer with pooled antiflagellin (polar and lateral) antibodies. Production of antibodies to polar and lateral flagellins has been described previously (41, 44). The secondary antibody was anti-rabbit immunoglobulin conjugated to horseradish peroxidase (Amersham Life Sciences). It was incubated with the blot at a dilution of 1:20,000 in TBST for 1 h. Development of the immunoblot utilized the chemiluminescent Super Signal substrate (Pierce) according to the manufacturer's instructions.

Motility assays and flagellum preparation. The effect of mutations on swimming motility was assessed by examining movement in M agar. Swarming motility was examined after inoculation on the surface of solidified swarming medium and overnight incubation. To examine swimming motility, plates were inoculated with 2 μl of cells normalized to an optical density at 600 nm of 2.0. Plates were incubated for the times indicated in legends to Fig. 4 to 6 and then refrigerated until photographed using a Kodak digital imaging system. Rates of radial expansion (in millimeters per hour) were determined in triplicate by measuring the diameter of expansion as a function of time. The slope was determined, and only lines with an R^2 value greater than 0.9 were used to calculate rates. All expansion rates were normalized to the rate of control strain LM1017, which was inoculated on the same plate. Flagella were isolated after shearing in a Virtis homogenizer, as described earlier (38).

Sequence analysis. Sequence determination was performed by the DNA Core Facility of the University of Iowa. Sequence assembly was accomplished using the Genetics Computer Group (GCG) software package. Searches for homology were performed at the National Center for Biotechnology Information with the BLAST network service (1). Multiple sequence alignments were performed using the CLUSTAL W program (58).

Nucleotide sequence accession number. The sequence obtained from clone pLM2047 for the *fliF* locus has been deposited with GenBank under accession no. AF069392.

RESULTS

Identification of genes encoding polar flagellar switch components. Strain ML199 is nonmotile and fails to produce a polar flagellum due to an insertion of the transposon mini-Mu (Tet^r). To determine the nature of the mutated gene, a restriction fragment containing part of the transposon encoding tetracycline resistance and the contiguous chromosomal DNA was cloned from strain ML199. Sequence analysis of the clone revealed that the transposon was inserted in a gene whose product was homologous to a protein involved in flagellar export, FlhA. Strain ML199 also contains a *lux* fusion in the lateral flagellar hook gene *lfgE*; thus it cannot swim or swarm. To test the effect of the *flhA* mutation on swarming, the lateral defect in ML199 was repaired using a cosmid carrying the *lfgE* locus. The resultant strain was competent for lateral flagellum production and swarming over solid surfaces but was unable to swim in semisolid motility medium (data not shown). Thus, the gene is pertinent to polar, but not lateral, flagellar assembly.

Sequencing upstream of the *flhA* gene revealed a large flagellar gene cluster, which included the three flagellar switch genes *fliG*, *fliM*, and *fliN*. The locus contains 15 potential flagellar genes. As depicted in Fig. 1, the genes are transcribed in the same direction and are tightly linked and the coding regions for many of the reading frames overlap with one an-

TABLE 1. Bacterial strains and plasmids

Strain or plasmid	Genotype or description	Source and/or parent; reference
Strains		
V. parahaemolyticus		
BB22	Wild type	R. Belas; 4
LM1017	*lfgE313*::*lux*	BB22; 44
LM4170	*motX118 lfgE313*::*lux*	LM1017; 40
LM4171	*motY141*::mini-Mu *lac lfgE313*::*lux*	LM1017; 39
LM4262	*motX1699*::Tn*phoA*	BB22; 40
LM4289	*motY1719*::Tn*phoA lfgE313*::*lux*	LM1017; 39
LM4474	*motY141*::mini-Mu *lac*	LM4171; this work
LM4652	*motA2*::Tn*phoA*	BB22; this work
LM4653	*motA3*::Tn*phoA*	BB22; this work
LM4654	*motB2*::Tn*phoA*	BB22; this work
LM4655	*motA1*::Tn*phoA*	BB22; this work
LM4656	*motB1*::Tn*phoA*	BB22; this work
LM4657	*motA2*::Tn*phoA lfgE313*::*lux*	LM1017; this work
LM4658	*motA3*::Tn*phoA lfgE313*::*lux*	LM1017; this work
LM4659	*motB2*::Tn*phoA lfgE313*::*lux*	LM1017; this work
LM4660	*motA1*::Tn*phoA lfgE313*::*lux*	LM1017; this work
LM4661	*motB1*::Tn*phoA lfgE313*::*lux*	LM1017; this work
LM4806	*fliG1*::Tn*lacZ*/in	BB22; this work
LM4807	*fliG1*::Tn*lacZ*/in *lfgE313*::*lux*	LM1017; this work
LM4808	*fliG2*::Tn*lacZ*/in	BB22; this work
LM4809	*fliG2*::Tn*lacZ*/in *lfgE313*::*lux*	LM1017; this work
LM4810	*fliG3*::Tn*lacZ*/in	BB22; this work
LM4811	*fliG3*::Tn*lacZ*/in *lfgE313*::*lux*	LM1017; this work
LM4812	*fliN1*::Tn*lacZ*/in *lfgE313*::*lux*	LM1017; this work
LM4813	*fliM2*::Tn*lacZ*/in	BB22; this work
LM4814	*fliM2*::Tn*lacZ*/in *lfgE313*::*lux*	LM1017; this work
LM4815	*fliM1*::Tn*lacZ*/in *lfgE313*::*lux*	LM1017; this work
LM4889	*fliM1*::Tn*lacZ*/in	BB22; this work
LM4890	*fliN1*::Tn*lacZ*/in	BB22; this work
E. coli		
DFB9	*thr(Am)1 leuB6 his4 metF(Am)159 thi1 rpsL136 Sm(R) lacY1 ara14 xyl5 mtl1 tsx78 tonA31 eda50*	D. Blair
DFB210	Δ*motAB*	DFB9, D. Blair
DFB223	Δ*fliN* (in frame)	DFB9, D. Blair
DFB225	Δ*fliG* (in frame)	DFB9, D. Blair
DFB228	Δ*fliM* (in frame)	DFB9, D. Blair
DFB232	Δ*fliMN* (in frame)	DFB9, D. Blair
Plasmids		
pBBR1MCS	Cam^r; broad-host-range vector	M. Kovach; 27
pLAFRII	Tet^r; broad-host-range cosmid vector	16
pMMB66EH	Ap^r; broad-host-range expression vector carrying $lacI^q$ and Ptac	17
pRK415	Tet^r; broad-host-range vector	24
pUCGM	Gen^r	H. Schweizer; 49
pLM1778	Tet^r; pLAFRII-derived cosmid carrying *lfgE* locus	This work
pLM1796	Tet^r; pLAFRII-derived cosmid carrying *lafTU* locus	44
pLM1877	Gen^r Ap^r; broad-host-range expression vector	pMMB66EH; this work
pLM2058	Tet^r;pLAFRII-derived cosmid carrying *motAB* locus	22
pLM2047	Tet^r; pLAFRII-derived cosmid carrying *fliF* locus	This work
pLM2192	Tet^r; $fliG^+H^+$	pRK415 and pLM2047; this work
pLM2293	Cam^r; $fliL^+M^+N^+O^+P^+$	pBBR1MCS and LM2047; this work
pLM2294	Gen^r; $fliM^+N^+$	pLM1877 and PCR product; this work
pLM2296	Gen^r; $fliM^+$	pLM1877 and PCR product; this work
pLM2297	Gen^r; $fliM^{short}$	pLM1877 and PCR product; this work

other. The sodium-type switch components resemble their proton-type homologs. For comparison, alignments with the *S. enterica* serovar Typhimurium gene products are shown in Fig. 2. Although the *V. parahaemolyticus* FliG protein possesses 20 additional amino acids at its amino terminus, the FliG proteins from the two organisms align without the introduction of significant gaps and display 55% similarity and 40% identity on the basis of a GCG BestFit alignment. The highest similarity occurs in the C-terminal domain: amino acids beyond residue 200 display 45% identity with the *S. enterica* serovar Typhimurium C-terminal domain. A number of residues in the C-terminal domain have been identified by mutational analysis of *E. coli* and *S. enterica* serovar Typhimurium to be functionally important for motor function (19, 29, 37), and these amino acids are conserved in *V. parahaemolyticus* FliG. The specific charged residues that have been shown to be critical for torque

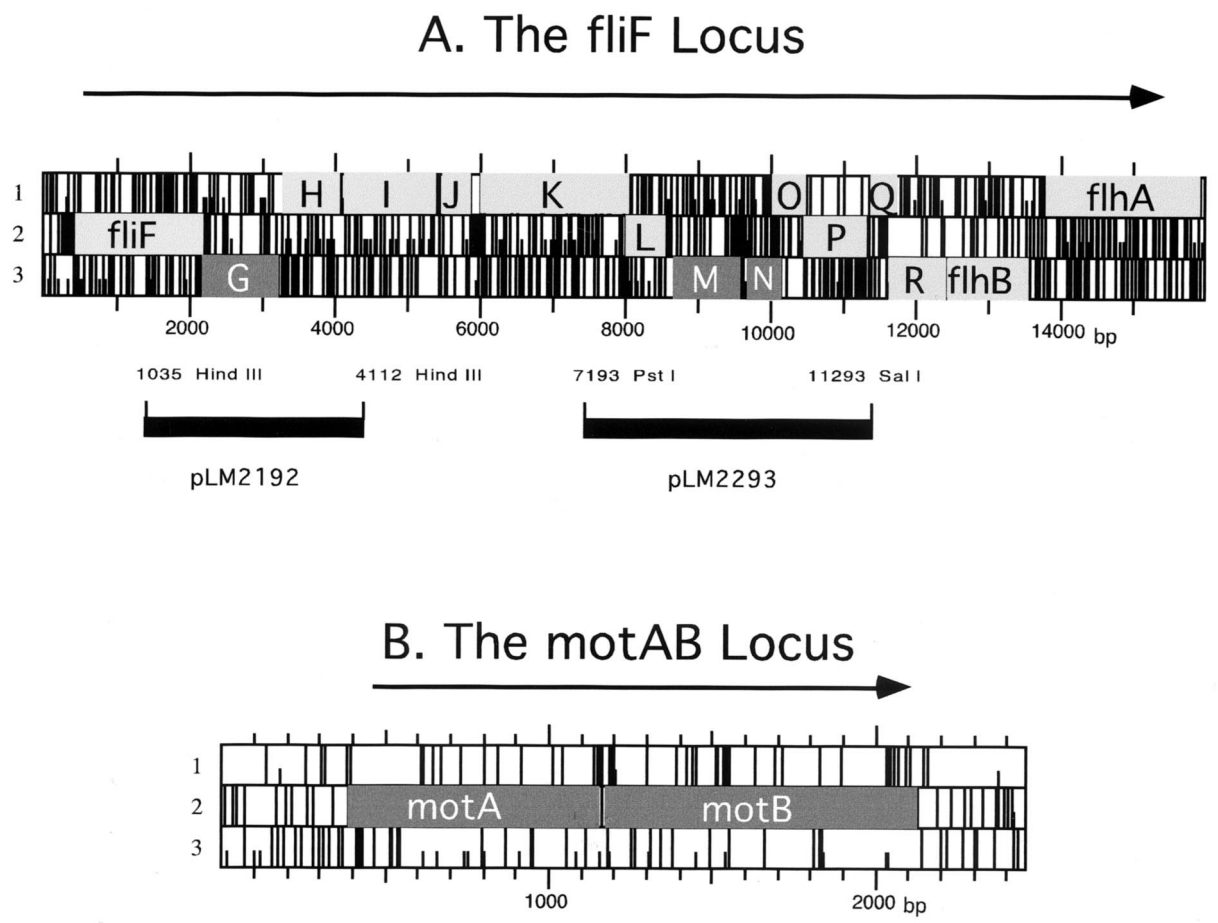

FIG. 1. The *fliF* and *motAB* loci. The physical maps are derived from the nucleotide sequences. Gene designations, which are adopted from the closest *E. coli* homolog, are superimposed on the open reading frame (ORF) map; full bars indicate stop codons, and small bars indicate ATG codons. ORFs coding for switch and motor genes are dark. Arrows indicate the direction of transcription. The coding sequence upstream of *fliF* codes for a potential transcriptional regulator resembling *E. coli* GcvA. The sequence upstream of *motA* codes for a potential polypeptide with homology to the small subunit of *E. coli* exodeoxyribonuclease (type VII). The sequence downstream of *motB* codes for a potential homolog of *S. enterica* serovar Typhimurium ThiI. Regions containing the *fliG* and *fliMN* genes were subcloned using the restriction sites indicated to make plasmids pLM2192 and pLM2293.

generation in *E. coli* FliG (29) and the positionally identical residues in *V. parahaemolyticus* FliG are indicated in Fig. 2A.

The predicted size of the *fliM* gene product is 348 residues. By using GCG BestFit analysis, it was found to be 52% similar and 37% identical with *S. enterica* serovar Typhimurium FliM over the first 320 amino acids. In particular, the N-terminal region, which for *S. enterica* serovar Typhimurium FliM has been shown to be critical for the interaction with phosphorylated CheY (61), is well conserved. Eight amino acid substitutions that produce motor-defective, i.e., paralyzed, flagella have been isolated in *S. enterica* serovar Typhimurium FliM (53). All of these amino acids are conserved between *S. enterica* serovar Typhimurium and *V. parahaemolyticus* (Fig. 1B). Seven of the eight are identical in the two organisms; the eighth is conserved with respect to charge (Arg in *V. parahaemolyticus* substituted for His in *S. enterica* serovar Typhimurium). In contrast to the conserved N-terminal region, the C terminus of the *V. parahaemolyticus* protein seems unusual. It is longer and more highly charged than any of the FliM sequences deposited in GenBank. The alignments of these proteins are without significant gaps over amino acids 1 through 320. A comparison of *V. parahaemolyticus* FliM with *S. enterica* serovar Typhimurium FliM is shown in Fig. 2B. Of the remaining 28 C-terminal amino acids beyond residue 320 of *V. parahaemolyticus* FliM, 14 possess charge, whereas only 3 of the remaining 12 C-terminal amino acids of *S. enterica* serovar Typhimurium are charged residues.

The predicted *fliN* gene product is 136 amino acids in length. It is 73% similar and 60% identical with *S. enterica* serovar Typhimurium FliN. Seven single-amino-acid substitutions that resulted in the paralyzed-Mot phenotype have been isolated within the *S. enterica* serovar Typhimurium gene (21). All of these residues (Fig. 2C) are identical between *S. enterica* serovar Typhimurium and *V. parahaemolyticus* except one (Thr substituted for Tyr). As was observed for *E. coli* (56), BLAST database searches with *V. parahaemolyticus* FliN reveal similarity with type III translocation proteins of the SpaO family (e.g., YopQ; GenBank accession no., 1176912). There is one significant gap in the alignment with *S. enterica* serovar Typhimurium FliN sequences. The predicted *V. parahaemolyticus* protein sequence possesses an insertion of five amino acids (Fig. 2C). All five of the inserted amino acids are charged residues.

Switch gene product identification. We were particularly interested in examining the protein product of *fliM* because of the unusual predicted C-terminal extension beyond residue

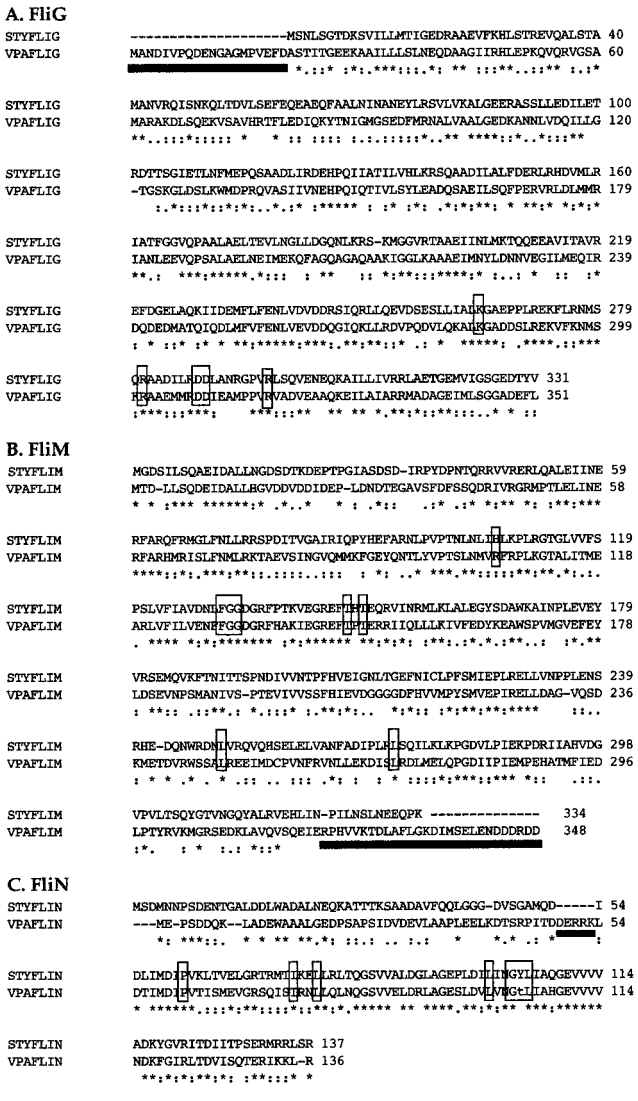

FIG. 2. Sequence alignment of sodium-type flagellar switch components of *V. parahaemolyticus* (VPA) with proton-type switch components of *S. enterica* serovar Typhimurium (STY). Amino acids are represented by the single-letter code. Gaps introduced to facilitate alignment are indicated by dashes. The consensus line below the sequence alignment indicates identity (*), strong conservation (:), and weak conservation (.) of amino acid matches. The open boxes outline conserved amino acids, and the lowercase letter indicates a nonconserved amino acid with respect to residues known to be critical for torque generation in *S. enterica* serovar Typhimurium or *E. coli*. Black bars underline the unusual domains of the *V. parahaemolyticus* proteins.

320. To do this, a plasmid was designed to encode a truncated FliM with 27 C-terminal amino acids deleted, FliM^{short}, which terminates at Arg-321. For *S. enterica* serovar Typhimurium, deletion of residues 321 to 334 produced a truncated FliM that fully supported motility (60). The *E. coli* minicell system was used to identify plasmid-encoded products. The plasmids contained coding sequence for FliM, FliN, and FliM^{short}, and the predicted molecular masses were 39,777, 14,964, and 36,709 Da, respectively. The autoradiogram of ^{35}S-labeled proteins is shown in Fig. 3. The FliM and FliN proteins migrated with apparent molecular masses of 43,500 and 21,500 Da, respectively. Both FliM and FliN are acidic proteins with predicted pIs of ~4.5, which may account for the apparently anomalous migration with respect to predicted mass in SDS-PAGE.

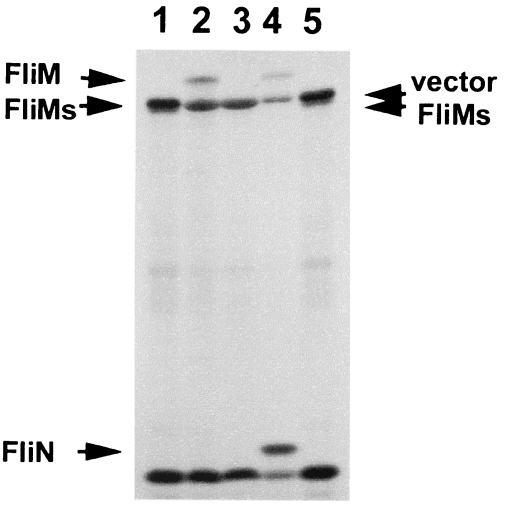

FIG. 3. FliM and FliN synthesis in minicells. Autoradiogram (12-h exposure) of ^{35}S-labeled proteins synthesized in minicells containing plasmids. Lanes: 1, pLM2297 (*fliM*^{short}); 2, pLM2296 (*fliM*$^{+}$); 3, pLM1877 (vector); 4, pLM2294 (*fliM*$^{+}$*N*$^{+}$); 5, pLM2297 (*fliM*^{short}). Arrows indicate polypeptides encoded by the *fli* genes and a vector-encoded product. The resolving gel contained 10.5% acrylamide. FliMs, the product of truncated *fliM*^{short}.

FliM^{short} migrated similarly to a protein product produced by the vector with an apparent molecular mass of ~41,200 Da.

Complementation of proton-type defective motor and switch mutants with sodium-type genes. The similarity between the sodium-type and proton-type switch components prompted investigation of protein function and interactions between heterologous motor parts. Clones containing *V. parahaemolyticus* motor and switch genes were transferred to *E. coli* strains with nonpolar defects in motor and switch genes. After extended incubation times, differences could be observed in M agar among *E. coli* strains DFB223 (Δ*fliN*), DFB228 (Δ*fliM*), and DFB232 (Δ*fliMN*) carrying the *fliF* locus on clone pLM2047 compared with those carrying a control vector. Figure 4A shows the effect of pLM2047 in DFB228 and DFB232 (strains 1 and 3 compared to strains 2 and 4), and the movement of strain DFB223 with pLM2047 was similar, but is not shown. Observation in the light microscope of strains with *fliM* and/or *fliN* defects and plasmid pLM2047 revealed cells that twitched or rotated in place without significant translocation. In contrast, no effect on motility could be observed in M agar or in the microscope for a strain with a *fliG* defect and pLM2047 (Fig. 4A, strain 5 compared to strain 6). Flagella could be isolated after shearing and high speed centrifugation for *fliM* or *fliN*, but not *fliG*, mutants carrying pLM2047. Immunoblots containing whole-cell samples probed with antiserum directed against *E. coli* flagellin revealed that *E. coli fliM* or *fliN* mutants containing cosmid pLM2047 produced approximately as much flagellin as a control *E. coli* strain that was wild type for motility, whereas no flagellin was detected in the *fliG* mutant containing pLM2047 (data not shown). Similarly, the polar *mot* gene products do not appear to compensate for *motAB* defects in *E. coli*: no motility was observed in M agar or in the microscope (Fig. 4B, strain 7). This was not an unexpected finding, for the degrees of similarity between the sodium-type MotA and MotB predicted polypeptides and the *E. coli* homologs were lower than those among the switch proteins. For comparison, complementation of the *E. coli* Δ*motAB* strain with the lateral, proton-type homologs of *V. parahaemolyticus* is shown (Fig. 4B, strain 8).

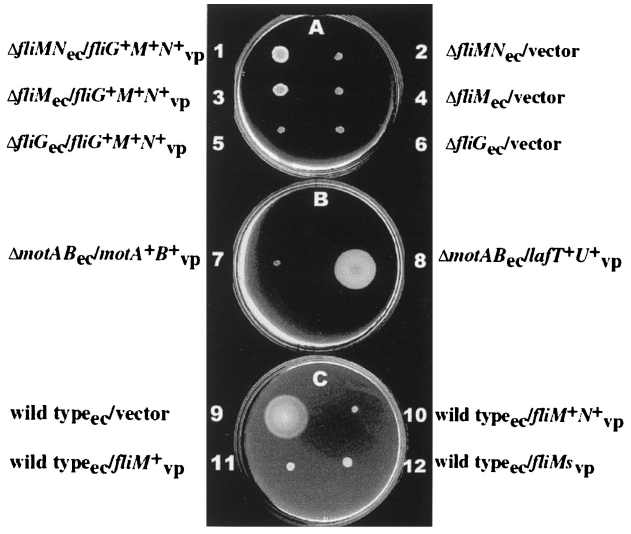

FIG. 4. Complementation experiments of *E. coli* (ec) proton-type motor and switch mutants with *V. parahaemolyticus* (vp) sodium-type genes. Strains: 1, DFB232 (Δ*fliMN*)/pLM2047 (containing *V. parahaemolyticus fliF* locus); 2, DFB232/pLAFRII (parental vector control); 3, DFB228 (Δ*fliM*)/pLM2047; 4, DFB228/pLAFRII; 5, DFB225 (Δ*fliG*)/pLM2047; 6, DFB225/pLAFRII; 7, DFB210 (Δ*motAB*)/pLM2058 (containing *V. parahaemolyticus motAB*); 8, DFB210/pLM1796 (containing the *V. parahaemolyticus lafTU* locus, which contains the lateral, proton-type motor genes); 9, DFB9 (wild type)/pLM1877; 10, DFB9/pLM2294; 11, DFB9/pLM2296; 12, DFB9/pLM2297. Plates A to C were incubated at 37°C for 60, 48, and 8 h, respectively. M agar in plates A and B contained 10 μg of tetracycline/ml for maintenance of the plasmids. M agar in plate C contained 40 μg of gentamicin/ml and 0.5 mM IPTG for induction of transcription of the *fli* genes contained on the expression vector pLM1877. *fliMs*, *fliM*^{short}.

Additional evidence supports the idea that certain proton- and sodium-type switch parts can interact, albeit not productively. The IPTG-inducible expression clones were introduced into motile strain DFB9. Induction of expression of *V. parahaemolyticus fliM*, *fliM*^{short}, or *fliMN* interfered with motility compared to what was found for DFB9 carrying the expression vector pLM1877 (Fig. 4C). Induction of expression had no effect on growth rates.

Transposon mutagenesis of switch and motor genes. Insertion mutations were isolated in each of the *V. parahaemolyticus* switch and motor genes, i.e., *fliG*, *fliM*, *fliN*, *motA*, and *motB*. Previously, transposon insertions had been isolated in the other identified motor genes, *motX* and *motY* (39, 40). The *motAB* locus was mutagenized with the transposon Tn*phoA*, which can serve as a probe for protein topology. Five insertions in *motA* or *motB* were analyzed. One in-frame fusion that produced a hybrid MotB-alkaline phosphatase protein was obtained. The fusion occurred at amino acid 308, which is very close to the end of the 316-amino-acid MotB polypeptide. The *fliG* subclone pLM2192 and *fliMN* subclone pLM2193 were mutagenized with a transposon suitable for isolating protein fusions to β-galactosidase, Tn*lacZ*/in. The precise location of each insertion, defined by DNA sequencing, is provided in Table 2.

Gene disruption via allelic replacement and effects on swimming. The transposons in *mot* and *fli* genes were transferred to the chromosome of *V. parahaemolyticus* strain LM1017 via allelic exchange. Strain LM1017 contains a *lfg*::*lux* fusion in the lateral flagellar hook operon. Thus, movement of LM1017 in M agar is solely the result of propulsion by the polar motility system. Movement in M agar of a set of representative mutants is shown in Fig. 5. For comparison, the previously constructed *motX* and *motY* mutant strains are included. Insertions in *motA*, *motB*, *motX*, *motY*, *fliG*, *fliM*, or *fliN* caused complete loss of motility.

TABLE 2. Insertion mutations in motor and switch genes

Allele	Comments	Location of insertion[b]	
		bp	aa
motA1::Tn*phoA*		576	58
motA2::Tn*phoA*		627	75
motA3::Tn*phoA*		1094	230
motB1::Tn*phoA*		2093	304
motB2::Tn*phoA*	Blue fusion[a], partial function	2103	308
fliG1::Tn*lacZ*/in	Blue fusion	2860	228
fliG2::Tn*lacZ*/in	Blue fusion	2878	234
fliG3::Tn*lacZ*/in		2536	120
fliM1::Tn*lacZ*/in		8613	23
fliM2::Tn*lacZ*/in	Blue fusion	9391	83
fliN1::Tn*lacZ*/in	Blue fusion	9740	33

[a] Blue fusion, insertion produced an active alkaline phosphatase or β-galactosidase fusion protein that was capable of converting the color of a chromogenic substrate to blue.

[b] Location of insertion is given according to the base pairs (bp) on the physical map presented in Fig. 1, which corresponds to the sequence deposited in GenBank, and to the amino acid codon (aa) perturbed by the position of the transposon. The predicted total numbers of amino acids in the polypeptides encoded by each gene are 253 (*motA*), 316 (*motB*), 351 (*fliG*), 248, (*fliM*), and 136 (*fliN*).

One mutant strain displayed some movement. The motility in M agar of LM4659, which contains the *phoA* fusion near the end of *motB*, is shown in Fig. 5, strain 11 and 12. The rate of radial expansion in M agar normalized to the rate of the parental strain, LM1017, was 0.38 ± 0.03. Previously, we constructed the mutant strain LM4289 using a Tn*phoA* insertion in *motY* that created a fusion to alkaline phosphatase after amino acid 289. Like the MotB hybrid protein, which lacks eight C-terminal amino acids, the MotY-alkaline phosphatase hybrid, which lacks four N-terminal amino acids, is functional and permits motility (Fig. 5, strain 13 and 14). The rate of radial expansion for LM4289 was indistinguishable from that for LM1017 (Fig. 5, strains 9 and 10). Thus, in terms of protein function within the motor complex, both MotB and MotY can accommodate C-terminal extensions of fused alkaline phosphatase. Both of these fusion proteins retain their putative peptidoglycan interaction domains.

To distinguish loss of specific gene function from potentially polar effects on downstream flagellar assembly genes, the *fli* mutants were analyzed for complementation. Plasmid pLM2192, containing only intact *fliG* and *fliH* genes, restored the swimming motility of the *fliG* mutant strains LM4807, LM4809, and LM4811 in motility plates containing chloramphenicol to select for retention of the chromosomal mutation and tetracycline to select for maintenance of the plasmid. Complementation of LM4811 is shown in Fig. 6A. To confirm that the observed motility was due to complementation and not recombination, segregation analysis after serial passage of the complemented, motile swarms in the absence of an antibiotic demonstrated that the cells that had lost the plasmid concomitantly lost motility. IPTG-inducible motility was observed after the introduction of the *fliMN* expression plasmid pLM2294 into *fliN* strain LM4812 (Fig. 6B, strain 2 versus strain 1) and *fliM* strain LM4815 (strain 4 versus strain 3). Thus, the *fliG*, *fliM*, and *fliN* genes play essential roles in swimming motility. It should be noted that for IPTG-promoted induction of *fli* gene expression from plasmids pLM2294 (*fliM*$^+$*N*$^+$) and pLM2296

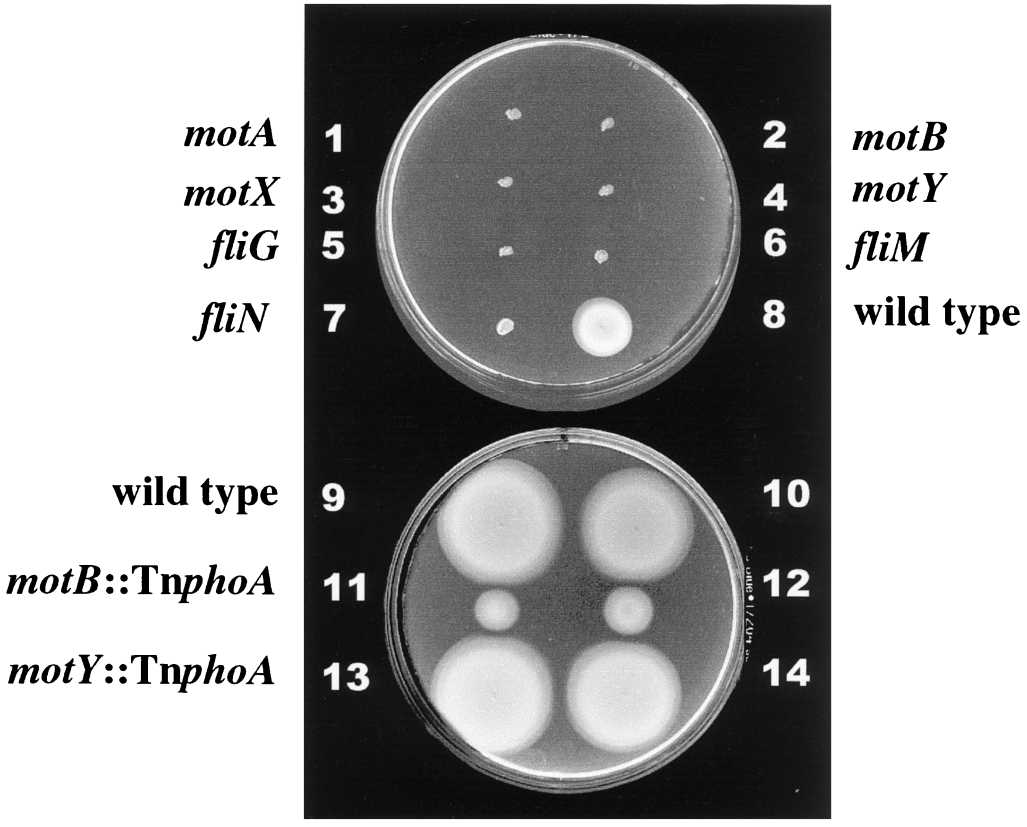

FIG. 5. Swimming motility of *V. parahaemolyticus* mutant strains with flagellar switch or motor defects in M agar. Strains: 1, LM4657 (*motA*); 2, LM4661 (*motB*); 3, LM4170 (*motX*); 4, LM4171 (*motY*); 5, LM4811 (*fliG*); 6, LM4815 (*fliM*); 7, LM4812 (*fliN*); 8, LM1017; 9 and 10, LM1017; 11 and 12, LM4659 (*motB2*::Tn*phoA*); 13 and 14, LM4289 (*motY1719*::Tn*phoA*). Semisolid motility plates were incubated at 30°C for 8 (top) and 9.5 h (bottom). All mutant strains are derivatives of LM1017. Strain LM1017 fails to produce lateral flagella; therefore, there is no contribution to motility from the lateral motility system.

(*fliN*$^+$), differences in motility for different mutant alleles were observed, e.g., insertions with Tn*phoA* aligned with or opposed to transcription and *fliM* versus *fliN* mutants. We interpret these data in light of findings for *E. coli* (56, 57) to suggest that the ratio of FliM to FliN is critical for maximal motility.

Introduction of pLM2296 (*fliM*$^+$) to strain LM4815 resulted in IPTG-controllable motility (Fig. 6B, strain 6); however, pLM2297 (containing *fliM*^{short}) failed to restore motility to LM4815 (strain 7). FliM^{short} appeared to interfere with flagellar assembly, for no flagellin was detected in immunoblots containing whole-cell preparations of IPTG-induced strain LM4815 with pLM2297 (data not shown). Moreover, IPTG induction of strain LM1017 with pLM2297, but not with the parental vector, pLM2296 (*fliM*$^+$), or pLM2294 (*fliM*$^+$*N*$^+$), reduced movement in M agar (Fig. 6B, strain 9 compared to strains 8, 10, and 11). This suggests that in *V. parahaemolyticus* *fliM*^{short} is expressed, the product is stable, and FliM^{short} negatively interferes with the function of the wild-type switch complex.

Effects of switch and motor mutations on swarming and swarmer cell gene expression. Although genetic evidence suggested that the *flhA* gene was required for polar but not lateral flagellar assembly, it seemed necessary to define the specificity of the roles of the upstream gene products, in particular, to determine whether the switch gene products were unique for polar motility or were shared by both flagellar systems. Gene disruption in the swarming-defective strain allowed evaluation of the role of the genes in swimming motility. To assess the contribution of the *fli* genes identified on cosmid pLM2047 to swarming motility, the transposons that were inserted into these genes were transferred to the chromosome of wild-type strain BB22.

Figure 7A shows polar and lateral flagellin profiles of wild-type and mutant strains harvested from plates. All of the strains produced lateral flagellin. The swarming motility over the surface of solidified swarm medium of strains with transposon-induced mutations in *motA*, *motB*, *motX*, *motY*, *fliG*, *fliM*, or *fliN* resembled wild-type swarming motility. Thus, lateral function is unaffected in the mutants, and these switch and motor genes are reserved for polar flagellar function. This panel also shows that mutant strains with *mot* defects produced polar flagellins, whereas strains with *fliG*, *fliM*, or *fliN* insertions failed to synthesize polar flagellins.

Previous work has demonstrated that polar flagellar function is intimately related to induction of swarmer cell development (38). Conditions that slow the flagellar motor down, e.g., solid surfaces, viscosity, or use of the sodium channel-blocking drug phenamil, induce swarmer cell development (23, 38). Genetic disruption of polar flagellar function has also been shown to result in constitutive swarmer cell gene expression (38, 41). To further dissect the mechanism of surface sensing and signal transmission, we examined the effect of these mutations, which knock out all known components of the polar motor, on induction of lateral flagella (Fig. 7B). In contrast to the wild-type strain, which only produces lateral flagella when grown on solidified medium (lane 9) and not when grown in liquid medium (lane 8), all of the mutants produced lateral flagella when grown in liquid culture (lanes 1 to 7).

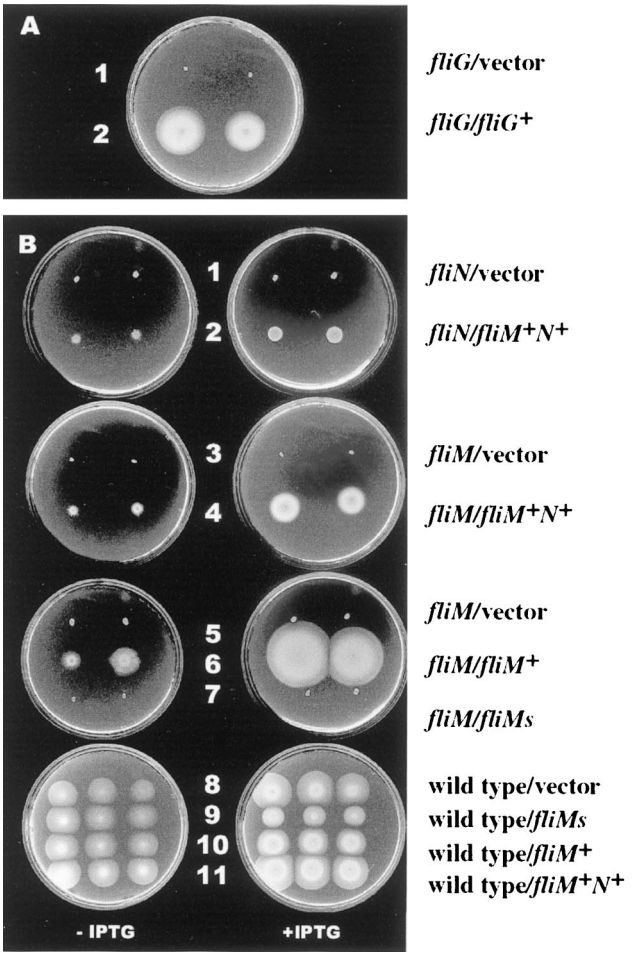

FIG. 6. Complementation of swimming motility defects in *V. parahaemolyticus* switch mutants with plasmids carrying *V. parahaemolyticus* switch genes. (A) Strains: 1, LM4811 (*fliG*)/pRK415 (vector); 2, LM4811 (*fliG*)/pLM2192 (*fliG*$^{+}$*H*$^{+}$). M agar was supplemented with 10 μg of chloramphenicol and 10 μg of tetracycline/ml. The plate was incubated for 16 h at 30°C. (B) Strains: 1, LM4812 (*fliN*)/pLM1877 (vector); 2, LM4812 (*fliN*)/pLM2294 (*fliM*$^{+}$*N*$^{+}$); 3, LM4815 (*fliM*)/pLM1877; 4, LM4815 (*fliM*)/pLM2294 (*fliM*$^{+}$*N*$^{+}$); 5, LM4815 (*fliM*)/pLM1877; 6, LM4815 (*fliM*)/pLM2296 (*fliM*$^{+}$); 7, LM4815 (*fliM*)/pLM2297 (*fliM*$^{short+}$); 8, LM1017/pLM1877 (vector); 9, LM1017/pLM2297 (*fliM*$^{short+}$); 10, LM1017/pLM2296 (*fliM*$^{+}$); 11, LM1017/pLM2294 (*fliM*$^{+}$*N*$^{+}$). M agar was supplemented with 10 μg of chloramphenicol/ml, 40 μg of gentamicin/ml, and 0.5 mM IPTG as indicated. Plates, from top to bottom, were incubated at 30°C for 14, 14, 19, and 10 h, respectively.

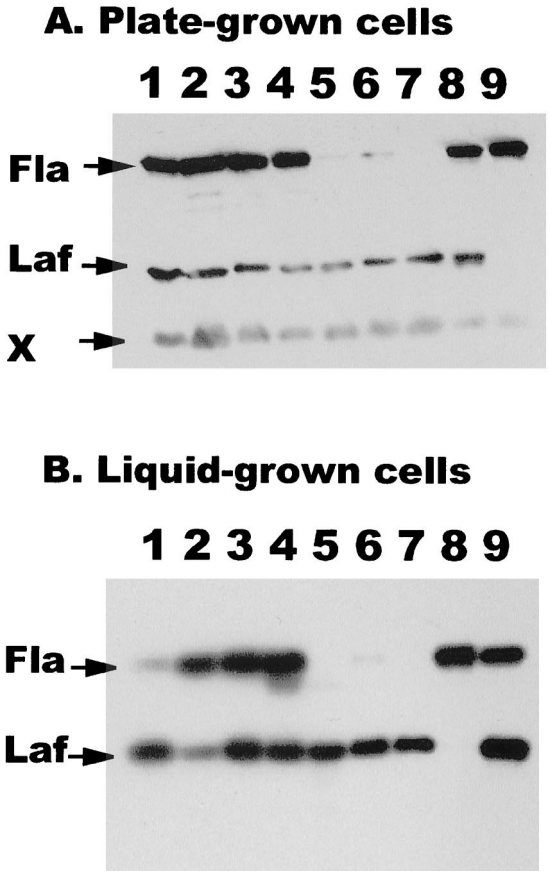

FIG. 7. Immunoblot analysis of polar and lateral flagellin production by strains with polar switch and motor defects. All mutant strains were derived from the wild-type strain BB22. Blots were reacted with pooled antisera directed against polar (Fla) and lateral (Laf) flagellins. (A) Mutant strains were harvested from plates. Lanes: 1, LM4652 (*motA*); 2, LM4656 (*motB*); 3, LM4262 (*motX*); 4, LM4474 (*motY*); 5, LM4810 (*fliG*); 6, LM4830 (*fliM*); 7, LM4832 (*fliN*); 8, BB22 (from plates); 9, BB22 (from liquid). (B) Strains harvested from liquid cultures were loaded into lanes as in panel A, except that lane 8 contained BB22 from liquid and lane 9 contained BB22 from plates. The immunoblot in panel A was reacted with pooled antisera at a dilution of 1:5,000 during an overnight incubation. A minor, antiserum-reactive, nonflagellin band (X) served as a control for the amount of whole cells loaded in each lane. The immunoblot in panel B was reacted with a 1:1,000 dilution of antilateral serum and a 1:5,000 dilution of antipolar serum for a 2-h incubation.

DISCUSSION

The rotary flagellar motor is a powerful molecular machine that couples the energy of membrane potential to rotation of the flagellum. This rotation is reversible, and the flagellum has been measured to turn at rates as fast as 100,000 rpm (33). The mechanism of conversion of chemical energy to work, i.e., transduction of the transmembrane potential of specific ions to generation of torque, is not fully understood. Two types of flagellar motors, driven by different coupling ions, are known. It is believed that there is highly efficient coupling of the passage of protons or sodium ions through the stationary part of the motor to the generation of torque (5), which occurs at the C ring found at the base of the flagellum. FliG, FliM, and FliN form the C ring of proton-type motors. The C ring is also known as the switch complex because it controls the direction of flagellar rotation. With respect to the proton-type motor, a structural model for the part of the rotor that interacts with the stator has been developed on the basis of extensive mutational analysis coupled with the crystal structure determination of the C-terminal domain of FliG (9, 18, 19, 21, 29, 31, 37, 50, 59). It is postulated that key charged residues on the face of a ridge of FliG interact with specific charged residues of MotA (31).

How does the sodium-type flagellar motor work? Seven components have been identified and are illustrated in Fig. 8. Four are membrane proteins and may comprise the stator. Two of these, MotB and MotY, possess domains likely to interact with peptidoglycan and may be the elements responsible for anchoring the force generator. These two proteins can be successfully fused to alkaline phosphatase with retention of function, which suggests that there is sufficient tolerance within the torque-generating complex to accommodate bulk near MotB and MotY. The proton-type motor has a single protein to perform the equivalent stabilizing function, i.e., MotB. In the proton-driven motor, transmembrane domains of MotA and MotB form the proton-conducting channel. For sodium-

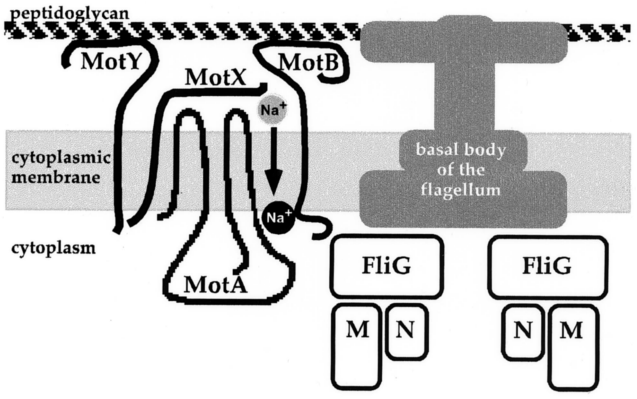

FIG. 8. Model for the sodium-type flagellar motor. Seven genes that encode components of the motor have been identified. Allelic disruption using transposons demonstrates that all are essential for polar-type motility. Alkaline phosphatase fusions at the C termini of MotB or MotY interfere with, but do not abolish, polar motility. The function of MotX is unknown, although it is essential for torque generation and has been shown to interact with MotY. MotA and MotB resemble their homologs in the proton-driven motor; although they are not interchangeable with the motor parts of *E. coli*. Potential Na^+ interaction sites on the cytoplasmic face of MotA and MotB (proximal to the Na^+ that is indicated by the black circle) have been defined by mutations conferring phenamil resistance. On passage of sodium ions through the motor, torque is transmitted from the presumed stationary components (MotA, -B, -X, and -Y) to the flagellar switch components (FliG, -M, and -N) located at the base of the flagellar basal body. Switch components are reserved for polar, and not lateral, function in *V. parahaemolyticus*, although they can partially interact with the *E. coli* flagellar apparatus.

driven motors, phenamil resistance maps to sites in MotA and MotB, implicating these proteins in Na^+ transfer (22, 26). The most unusual component of the motor is MotX, and its function is unknown, although it has been shown to recruit MotY to the membrane (40). When MotX is introduced into *E. coli*, its overexpression renders *E. coli* sensitive to killing by Na^+. Potentially MotX might modify or specify MotA-MotB ion channel selectivity. It is postulated that on transfer of Na^+ through the torque generator, force is transmitted from the stator to FliG, which is part of the rotor. Our discovery of the genes encoding components of the switching apparatus for the polar flagellum of *V. parahaemolyticus* provides insight into the workings of the sodium-type motor. The strong homology of the *V. parahaemolyticus fliG*, *fliM*, and *fliN* gene products with the proton-type switch proteins argues that the role of the switch complex in the sodium-type motor is similar to the role of the switch complex in the proton-type motor.

The deduced switch proteins of *V. parahaemolyticus* resemble their proton-type homologs. Each possesses conserved, charged residues previously shown to be required for motor function in *E. coli* and *S. enterica* serovar Typhimurium. The conservation of charged residues at the active-site ridge of proton-type FliG with residues in sodium-type FliG, coupled with the conservation of *E. coli* MotA residues shown to participate in key electrostatic interactions with FliG and amino acids in sodium-type MotA (22), suggests that the mechanisms of energy transfer at the rotor-stator interface in the two motors are similar, despite being powered by different ion flows.

In switch-defective *E. coli* mutant strains, low-level expression of *V. parahaemolyticus fliM* and *fliN*, but not *fliG*, induces trails of motility in M agar and the aberrant twitching motility observed in the microscope. High-level expression of *Vibrio fliM* or *fliN* impedes movement of the wild-type *E. coli* strain. Thus, when the sodium switch parts are expressed in *E. coli*, there is limited interaction between them and the proton-type motor-switch complex. *V. parahaemolyticus* FliG is unable to participate in the *E. coli* switching apparatus. The *E. coli* mutant with *Vibrio fliG* on a plasmid fails to produce flagella. It seems possible that the N-terminal domain of *V. parahaemolyticus* FliG precludes interaction with the *E. coli* switch-assembly complex. Studies with FliG of *Thermotoga maritima* have shown that although the full-length protein fails to interact properly with flagellar proteins of *E. coli*, replacement of the *T. maritima* FliG N terminus, which contains the domain required for flagellar assembly, with the equivalent domain from *E. coli* creates a functional hybrid protein (31). Sequence alignments of the C termini of *T. maritima* FliG and *V. parahaemolyticus* FliG exhibit the same degree of identity with *E. coli* FliG.

V. parahaemolyticus FliM and FliN possess charge domains not found in their proton-type counterparts. It will be of interest to determine whether these domains are functionally important and if so whether they are important with respect to motor, switching, or assembly function. To initiate such studies, we examined the C terminus of the FliM. C-terminal truncation of *S. enterica* serovar Typhimurium FliM does not impair protein function (60). On the basis of the nucleotide sequence, the *V. parahaemolyticus* FliM polypeptide was predicted to be more highly charged and longer than other FliM homologs. FliM production was examined in minicells, along with the product of truncated gene *fliM*^{short}, which coded for a protein prematurely terminating at residue 320. In contrast to what was found for a plasmid encoding full-length FliM, FliM^{short} failed to productively substitute when the truncated gene was introduced into *V. parahaemolyticus fliM* mutant strains, and mutant *fliM*/*fliM*^{short} merodiploid strains appear blocked in flagellar assembly for they failed to produce flagellin. FliM^{short} negatively interfered with motility when overexpressed from a plasmid in the wild-type strain. Taken together, these experiments support the idea that the charged C terminus of *V. parahaemolyticus* FliM is essential for motility.

V. parahaemolyticus achieves the assembly of two types of flagellar appendages simultaneously. Prior genetic analysis has suggested, but not proven, that polar and lateral flagellar structural and assembly components were distinct because mutants failing to swim could still swarm and vice versa (38, 42). However, when both flagellar systems are present, behavior is coordinated; therefore, at some level the two motility systems must be integrated. How is the flow of chemosensory information channeled? It is known that chemotaxis mutants with defects in a locus that encodes central, chemotaxis signal transduction proteins fail to productively swim or swarm (48). This work identifies a large locus of flagellar genes that encode components for the switching apparatus and assembly. Insertional inactivation of *fliG*, *fliM*, and *fliN* genes in this locus demonstrated that the genes encode products reserved for polar function. All of the mutants retained swarming motility. Thus, these switch genes are specialized for the polar system. It seems that integration of chemosensory signaling must occur prior to interaction with the switch. Perhaps phosphorylated CheY can interact with both polar and lateral switch complexes, or perhaps multiple CheY proteins exist. Recent studies have shown that a domain near the N terminus of *S. enterica* serovar Typhimurium FliM interacts with phospho-CheY (61), and this segment is quite well conserved in the *V. parahaemolyticus* polar FliM. The switch components for the *Vibrio* lateral motor remain to be identified.

This work also provides some insight into the hierarchy of polar flagellar gene control and assembly. Mutants with defects in the polar motor genes, *motX*, *motY*, *motA*, and *motB*, produce a polar flagellum, as determined by immunodetection of flagellins (shown in this work) and electron microscopy (not

shown). Thus, the *mot* products are not required for flagellar assembly. Mutants with defects in the *fliG*, *fliM*, or *fliN* gene fail to produce polar flagellins. Immunoblot analysis of flagellin production was performed on whole cells; therefore, flagellin gene expression seems to also be affected. These results are consistent with the hierarchy of flagellar gene control and assembly that has been established for *E. coli* and *S. enterica* serovar Typhimurium (32). In addition, the phenotype of these mutants contributes to our understanding of the mechanism of surface sensing. The performance of the polar flagellum is coupled to the transcription of swarmer cell genes. When function is inhibited, for example, by physical constraint (38) or by using the sodium channel inhibitor phenamil (23), swarmer cell differentiation is induced. Polar flagellar rotation and swarmer cell induction are inversely correlated, and thus motor function is implicated in signal transduction. We have now determined that loss of function of any of the seven motor or switch genes creates mutant strains constitutive for expression of swarmer cell genes. Thus, none of these gene products are essential for triggering swarmer cell development.

ACKNOWLEDGMENTS

We thank David Blair for bacterial strains and counsel, May Macnab for antiserum to *E. coli* flagellin, and the DNA Core at the University of Iowa for excellent support.

This research was supported by Public Health Service grant GM43196 from the National Institutes of Health to L.L.M. and NSF and Howard Hughes Undergraduate Research Fellowships to B.R.B.

REFERENCES

1. **Altschul, S. F., T. L. Madden, A. A. Schaffer, J. Zhang, Z. Zhang, W. Miller, and D. J. Lipman.** 1997. Gapped BLAST and PSI-BLAST: a new generation of protein database search programs. Nucleic Acids Res. **25:**3389–3402.
2. **Asai, Y., S. Kojima, H. Kato, N. Nishioka, I. Kawagishi, and M. Homma.** 1997. Putative channel components for the fast-rotating sodium flagellar motor of a marine bacterium. J. Bacteriol. **179:**5104–5110.
3. **Atsumi, T., L. McCarter, and Y. Imae.** 1992. Polar and lateral flagellar motors of marine *Vibrio* are driven by different ion membrane forces. Nature (London) **355:**182–184.
4. **Belas, R., M. Simon, and M. Silverman.** 1986. Regulation of lateral flagella gene transcription in *Vibrio parahaemolyticus*. J. Bacteriol. **167:**210–218.
5. **Berg, H. C.** 1995. Torque generation by the flagellar rotary motor. Biophys. J. **68:**163s–167s.
6. **Blair, D. F.** 1995. How bacteria sense and swim. Annu. Rev. Microbiol. **49:**489–522.
7. **Blair, D. F., and H. C. Berg.** 1990. The MotA protein of *E. coli* is a proton-conducting component of the flagellar motor. Cell **60:**439–449.
8. **Blair, D. F., and H. C. Berg.** 1991. Mutations in the MotA protein of *Escherichia coli* reveal domains critical for proton conduction. J. Mol. Biol. **221:**1433–1442.
9. **Braun, T. F., S. Poulson, J. B. Gully, J. C. Empey, S. V. Way, A. Putnam, and D. F. Blair.** 1999. Function of proline residues of MotA in torque generation by the flagellar motor of *Escherichia coli*. J. Bacteriol. **181:**3542–3551.
10. **Chun, S. Y., and J. S. Parkinson.** 1988. Bacterial motility: membrane topology of the *Escherichia coli* MotB protein. Science **230:**276–277.
11. **Dean, G. E., R. M. Macnab, J. Stader, P. Matsumura, and C. Burks.** 1984. Gene sequence and predicted amino acid sequence of the *motA* protein, a membrane-associated protein required for flagellar rotation in *Escherichia coli*. J. Bacteriol. **159:**991–999.
12. **DeMot, R., and J. Vanderleyden.** 1994. The C-terminal sequence conservation between OmpA-related outer membrane proteins and MotB suggests a common function in both Gram-positive and Gram-negative bacteria, possibly in the interaction of these domains with peptidoglycan. Mol. Microbiol. **12:**333–334.
13. **DeRosier, D. J.** 1998. The turn of the screw: the bacterial flagellar motor. Cell **93:**17–20.
14. **Engebrecht, J., and M. Silverman.** 1984. Identification of genes and gene products necessary for bacterial bioluminescence. Proc. Natl. Acad. Sci. USA **81:**4154–4158.
15. **Francis, N. R., G. E. Sosinsky, D. Thomas, and D. J. DeRosier.** 1994. Isolation, characterization and structure of bacterial flagellar motors containing the switch complex. J. Mol. Biol. **235:**1261–1270.
16. **Friedman, A., S. R. Long, S. E. Brown, W. J. Buikema, and F. Ausubel.** 1982. Construction of a broad host range cosmid cloning vector and its use in the genetic analysis of *Rhizobium* mutants. Gene **18:**289–296.
17. **Fuerste, J. P., W. Pansegrau, R. Frank, H. Blocker, P. Scholz, M. Bagdasarian, and E. Lanka.** 1986. Molecular cloning of the plasmid RP4 primase region in a multi-host-range *tacP* expression vector. Gene **48:**119–131.
18. **Garza, A. G., R. Biran, J. A. Wohlschlegel, and M. D. Manson.** 1996. Mutations in *motB* suppressible by changes in stator or rotor components of the bacterial flagellar motor. J. Mol. Biol. **258:**270–285.
19. **Garza, A. G., L. W. Harris-Haller, R. A. Stoebner, and M. D. Manson.** 1995. Motility protein interactions in the bacterial flagellar motor. Proc. Natl. Acad. Sci. USA **92:**1970–1974.
20. **Imae, Y., and T. Atsumi.** 1989. Na^+ driven bacterial flagellar motors. J. Bioenerg. Biomembr. **21:**705–716.
21. **Irikura, V. M., M. Kihara, S. Yamaguchi, H. Sockett, and R. M. Macnab.** 1993. *Salmonella typhimurium fliG* and *fliN* mutations causing defects in assembly, rotation, and switching of the flagellar motor. J. Bacteriol. **175:**802–810.
22. **Jaques, S., Y.-K. Kim, and L. L. McCarter.** 1999. Mutations conferring resistance to phenamil and amiloride, inhibitors of sodium-driven motility of *Vibrio parahaemolyticus*. Proc. Natl. Acad. Sci. USA **96:**5740–5745.
23. **Kawagishi, I., M. Imagawa, Y. Imae, L. McCarter, and M. Homma.** 1996. The sodium-driven polar flagellar motor of marine *Vibrio* as the mechanosensor that regulates lateral flagellar expression. Mol. Microbiol. **20:**693–699.
24. **Keen, N. T., S. Tamaki, D. Kobayashi, and D. Trollinger.** 1988. Improved broad-host-range plasmids for DNA cloning in gram-negative bacteria. Gene **70:**191–197.
25. **Khan, S., M. Dapice, and T. S. Reese.** 1988. Effects of *mot* gene expression on the structure of the flagellar motor. J. Mol. Biol. **202:**575–584.
26. **Kojima, S., Y. Asai, T. Atsumi, I. Kawagishi, and M. Homma.** 1999. Na^+-driven flagellar motor resistant to phenamil, an amiloride analog, caused by mutations in putative channel components. J. Mol. Biol. **285:**1537–1547.
27. **Kovach, M. E., R. W. Phillips, P. H. Elzer, R. M. Roop II, and K. M. Peterson.** 1994. PBBR1MCS: a broad-host-range cloning vector. BioTechniques **16:**800–802.
28. **Larsen, S. H., J. Adler, J. J. Gargus, and R. W. Hogg.** 1974. Chemomechanical coupling without ATP: the source of energy for motility and chemotaxis in bacteria. Proc. Natl. Acad. Sci. USA **71:**1239–1243.
29. **Lloyd, S. A., and D. F. Blair.** 1997. Charged residues of the rotor protein FliG essential for torque generation in the flagellar motor of *Escherichia coli*. J. Mol. Biol. **266:**733–744.
30. **Lloyd, S. A., H. Tang, X. Wang, S. Billings, and D. F. Blair.** 1996. Torque generation in the flagellar motor of *Escherichia coli*: evidence of a direct role for FliG but not for FliM or FliN. J. Bacteriol. **178:**223–231.
31. **Lloyd, S. A., F. G. Whitby, D. F. Blair, and C. P. Hill.** 1999. Structure of the C-terminal domain of FliG, a component of the rotor in the bacterial flagellar motor. Nature **400:**472–475.
32. **Macnab, R. M.** 1996. Flagella and motility, p. 123–146. *In* F. C. Neidhardt, R. Curtiss, III, J. L. Ingraham, E. C. C. Lin, K. B. Low, B. Magasanik, W. S. Reznikoff, M. Riley, M. Schaechter, and H. E. Umbarger (ed.), *Escherichia coli* and *Salmonella*: cellular and molecular biology, 2nd ed. ASM Press, Washington, D.C.
33. **Magariyama, Y., S. Sugiyama, K. Muramoto, Y. Maekawa, I. Kawagishi, Y. Imae, and S. Kudo.** 1994. Very fast flagellar rotation. Nature **371:**752.
34. **Manoil, C., and J. Bailey.** 1997. A simple screen for permissive sites in proteins: analysis of *Escherichia coli lac* permease. J. Mol. Biol. **267:**250–263.
35. **Manoil, C., and J. Beckwith.** 1985. Tn*phoA*: a transposon probe for protein export signals. Proc. Natl. Acad. Sci. USA **83:**8129–8133.
36. **Manson, M. D., P. Tedesco, H. C Berg, F. M. Harold, and C. van der Drift.** 1977. A protonmotive force drives bacterial flagella. Proc. Natl. Acad. Sci. USA **74:**3060–3064.
37. **Marykwas, D. L., and H. C. Berg.** 1996. A mutational analysis of the interaction between FliG and FliM, two components of the flagellar motor of *Escherichia coli*. J. Bacteriol. **178:**1289–1294.
38. **McCarter, L., M. Hilmen, and M. Silverman.** 1988. Flagellar dynamometer controls swarmer cell differentiation of *V. parahaemolyticus*. Cell **54:**345–351.
39. **McCarter, L. L.** 1994. MotY, a component of the sodium-type flagellar motor. J. Bacteriol. **176:**4219–4225.
40. **McCarter, L. L.** 1994. MotX, a channel component of the sodium-type flagellar motor. J. Bacteriol. **176:**5988–5998.
41. **McCarter, L. L.** 1995. Genetic and molecular characterization of the polar flagellum of *Vibrio parahaemolyticus*. J. Bacteriol. **177:**1595–1609.
42. **McCarter, L. L.** 1999. The multiple identities of *Vibrio parahaemolyticus*. J. Mol. Microbiol. Biotechnol. **1:**51–57.
43. **McCarter, L. L., and M. Silverman.** 1987. Phosphate regulation of gene expression in *Vibrio parahaemolyticus*. J. Bacteriol. **169:**3441–3449.
44. **McCarter, L. L., and M. E. Wright.** 1993. Identification of genes encoding components of the swarmer cell flagellar motor and propeller and a sigma factor controlling differentiation of *Vibrio parahaemolyticus*. J. Bacteriol. **175:**3361–3371.
45. **Meister, M., G. Lowe, and H. C. Berg.** 1987. The proton flux through the bacterial flagellar motor. Cell **49:**643–650.
46. **Oosawa, K., T. Ueno, and S. I. Aizawa.** 1994. Overproduction of the bacterial

flagellar switch proteins and their interactions with the MS ring complex in vitro. J. Bacteriol. **176:**3683–3691.
47. **Sambrook, J., E. F. Fritsch, and T. Maniatis.** 1989. Molecular cloning: a laboratory manual, 2nd ed. Cold Spring Harbor Laboratory, Cold Spring Harbor, N.Y.
48. **Sar, N., L. McCarter, M. Simon, and M. Silverman.** 1990. Chemotactic control of the two flagellar systems of *Vibrio parahaemolyticus*. J. Bacteriol. **172:**334–341.
49. **Schweizer, H. P.** 1993. Small broad-host-range gentamicin resistance gene cassette for site-specific insertion and deletion mutagenesis. BioTechniques **15:**831–833.
50. **Sharp, L. L., J. Zhou, and D. F. Blair.** 1995. Tryptophan-scanning mutagenesis of MotB, an integral membrane protein essential for flagellar rotation in *Escherichia coli*. Biochemistry **34:**9166–9171.
51. **Sharp, L. L., J. Zhou, and D. F. Blair.** 1995. Features of MotA proton channel structure revealed by tryptophan-scanning mutagenesis. Proc. Natl. Acad. Sci. USA **92:**7946–7950.
52. **Silverman, M., R. Showalter, and L. McCarter.** 1991. Genetic analysis in *Vibrio*. Methods Enzymol. **204:**515–536.
53. **Sockett, H., S. Yamaguchi, M. Kihara, V. M. Irikura, and R. M. Macnab.** 1992. Molecular analysis of the flagellar switch protein FliM of *Salmonella typhimurium*. J. Bacteriol. **174:**793–806.
54. **Stader, J., P. Matsumura, D. Vacante, G. E. Dean, and R. M. Macnab.** 1986. Nucleotide sequence of the *Escherichia coli motB* gene and site-limited incorporation of its product into the cytoplasmic membrane. J. Bacteriol. **166:**244–252.
55. **Stolz, B., and H. C. Berg.** 1991. Evidence for interactions between MotA and MotB, torque-generating elements of the flagellar motor of *Escherichia coli*. J. Bacteriol. **173:**7033–7037.
56. **Tang, H., S. Billings, X. Wang, L. Sharp, and D. F. Blair.** 1995. Regulated underexpression and overexpression of the FliN protein of *Escherichia coli* and evidence for an interaction between FliN and FliM in the flagellar motor. J. Bacteriol. **177:**3496–3503.
57. **Tang, H., and D. F. Blair.** 1995. Regulated underexpression of the FliM protein of *Escherichia coli* and evidence for location in the flagellar motor distinct from the MotA/MotB torque generators. J. Bacteriol. **177:**3485–3495.
58. **Thompson, J. D., D. G. Higgins, and T. J. Gibson.** 1994. CLUSTAL W: improving the sensitivity of progressive multiple sequence alignment through sequence weighting, position-specific gap penalties and weight matrix choice. Nucleic Acids Res. **22:**4673–4680.
59. **Togashi, F., S. Yamaguchi, M. Kihara, S.-I. Aizawa, and R. M. Macnab.** 1997. An extreme clockwise switch bias mutation in *fliG* of *Salmonella typhimurium* and its suppression by slow-motile mutations in *motA* and *motB*. J. Bacteriol. **179:**2994–3003.
60. **Toker, A. S., M. Kihara, and R. M. Macnab.** 1996. Deletion analysis of the *fliM* flagellar switch protein of *Salmonella typhimurium*. J. Bacteriol. **178:** 7069–7079.
61. **Toker, A. S., and R. M. Macnab.** 1997. Distinct regions of bacterial flagellar switch protein FliM interact with FliG, FliN, and CheY. J. Mol. Biol. **273:** 623–634.
62. **Welch, M., K. Oosawa, S.-I. Aizawa, and M. Eisenbach.** 1993. Phosphorylation-dependent binding of a signal molecule to the flagellar switch of bacteria. Proc. Natl. Acad. Sci. USA **90:**8787–8791.
63. **Woo, T. H. S., A. F. Cheng, and J. M. Ling.** 1992. An application of a simple method for the preparation of bacterial DNA. BioTechniques **13:**696–697.
64. **Yamaguchi, S., H. Fujita, A. Ishihara, S.-I. Aizawa, and R. M. Macnab.** 1986. Subdivision of flagellar genes of *Salmonella typhimurium* into regions responsible for assembly, rotation, and switching. J. Bacteriol. **166:**187–193.
65. **Yamaguchi, S., S.-I. Aizawa, M. Kihara, M. Isomura, C. J. Jones, and R. M. Macnab.** 1986. Genetic evidence for a switching and energy-transducing complex in the flagellar motor of *Salmonella typhimurium*. J. Bacteriol. **168:**1172–1179.
66. **Zhou, J., and D. F. Blair.** 1997. Residues of the cytoplasmic domain of MotA essential for torque generation in the bacterial flagellar motor. J. Mol. Biol. **273:**428–439.
67. **Zhou, J., S. A. Lloyd, and D. F. Blair.** 1998. Electrostatic interactions between rotor and stator in the bacterial flagellar motor. Proc. Natl. Acad. Sci. USA **95:**6436–6441.
68. **Zhou, J., L. L. Sharp, H. L. Tan, S. A. Lloyd, S. Billings, T. F. Braun, and D. F. Blair.** 1998. Function of protonable residues in the flagellar motor of *Escherichia coli*: a critical role for Asp 32 of MotB. J. Bacteriol. **180:**2729–2735.